

Robust Principal Component Analysis: A Median of Means Approach

Debolina Paul¹, Saptarshi Chakraborty^{*2}, and Swagatam Das^{3,4}

¹Department of Statistics, Stanford University

²Department of Statistics, University of California, Berkeley

³Electronics and Communication Sciences Unit, Indian Statistical Institute, Kolkata, India

⁴Institute for Advancing Intelligence (IAI), TCG CREST, Kolkata India

July 21, 2023

Abstract

Principal Component Analysis (PCA) is a fundamental tool for data visualization, denoising, and dimensionality reduction. It is widely popular in Statistics, Machine Learning, Computer Vision, and related fields. However, PCA is well-known to fall prey to outliers and often fails to detect the true underlying low-dimensional structure within the dataset. Following the Median of Means (MoM) philosophy, recent supervised learning methods have shown great success in dealing with outlying observations without much compromise to their large sample theoretical properties. This paper proposes a PCA procedure based on the MoM principle. Called the Median of Means Principal Component Analysis (MoMPCA), the proposed method is not only computationally appealing but also achieves optimal convergence rates under minimal assumptions. In particular, we explore the non-asymptotic error bounds of the obtained solution via the aid of the Rademacher complexities while granting absolutely no assumption on the outlying observations. The derived concentration results are not dependent on the dimension because the analysis is conducted in a separable Hilbert space, and the results only depend on the fourth moment of the underlying distribution in the corresponding norm. The proposal's efficacy is also thoroughly showcased through simulations and real data applications.

1 Introduction

Principal component analysis (PCA) [1, 2] is perhaps the most well-known statistical method for linear dimensionality reduction [3]. Given a set of (mean-centered) points $\mathcal{X} = \{\mathbf{x}_1, \dots, \mathbf{x}_N\} \subset \mathbb{R}^p$, the PCA computes a small number of orthonormal basis vectors, which characterize most of the variability within the data cloud. Mathematically, to find a d -dimensional ($d \leq p$) representation of \mathcal{X} , one projects these N points on to a d -dimensional subspace as $\{\mathbf{Q}\mathbf{x}_1, \dots, \mathbf{Q}\mathbf{x}_N\}$. where, \mathbf{Q} is a $p \times p$ projection matrix of rank d . Denoting the set of all $p \times p$ projection matrices of rank d as \mathcal{Q}_d , the PCA minimizes the following objective:

$$\frac{1}{N} \sum_{i=1}^N \|\mathbf{x}_i - \mathbf{Q}\mathbf{x}_i\|^2 = \frac{1}{N} \sum_{i=1}^N \mathbf{x}_i^\top (\mathbf{I} - \mathbf{Q}) \mathbf{x}_i, \quad (1)$$

*Correspondence to: saptarshic@berkeley.edu.

where $\mathbf{Q} \in \mathcal{Q}_d$.

Though efficient in many real-life scenarios, PCA is well documented to suffer from many disadvantages such as information loss, poor performance when the data lies in a non-affine manifold, poor performance for high-dimensional data, etc. Researchers continue to tackle these issues through modifications to the original versions, such as probabilistic PCA [4], kernel PCA [5], sparse PCA [6], robust PCA [7, 8], and so on. Among many disadvantages of PCA, like information loss and poor interpretation, one of the major concerns is that it is well known to fail in the presence of a single outlying observation. Its fragility against severely corrupted data points often puts its reliability at risk. Popular approaches for making the PCA more robust to these outlying and corrupted observations attempt to represent the original data matrix \mathbf{x} as a sum of a low-rank matrix \mathbf{L} and a sparse matrix \mathbf{S} [7, 9, 10, 11, 12, 13, 14]. However, many methods mentioned earlier only allow recovery guarantees under very restrictive assumptions. For example, [7] restricts the structure of \mathbf{S} to a Bernoulli model.

Robust PCA has recently gained popularity, primarily due to the rise of Big Data. These big datasets often contain outliers and hence require delicate handling, usually done by implementing robust statistics against outlying observations. Recently, there has been much interest in the robust dimensionality reduction community on proposing efficient frameworks for PCA [15, 16, 17]. There has also been an array of work based on geometric median-based approaches [18, 19, 20, 21], which focuses on a robust estimation of the covariance matrix and finding the eigendecomposition of the same to find the proper subspace to project. Although efficient in practice, many techniques mentioned above do not come with finite-sample theoretical guarantees. Those with asymptotic rates often assume that the data points are independent and identically distributed, which does not hold when the data is contaminated with outliers.

To bridge this methodological gap, the Median of Means (MoM) literature provides a promising and attractive framework to adapt PCA to become outlier robust, as well as help us preserve our theoretical understanding of finite-sample error bounds. As opposed to the classical Vapnik-Chervonenkis Empirical Risk Minimization (ERM) [22], the MoM philosophy provides a more robust framework for efficiently finding estimates of the actual underlying parameter. Although MoM estimators have been in the literature for quite a long time, it has recently been introduced to the Machine learning community [23, 24, 25, 26]. Besides being insensitive to outliers, the MoM estimators also possess a solid theoretical backbone comprising exponential concentration results under the mild restriction of finite variance [23, 24, 25, 27, 28]. Recently, several near-optimal results were established from this perspective concerning regression [23, 29], bandits [30], mean estimation [31], clustering [32, 33, 34], classification [35], and optimal transport [36].

In this paper, we develop a Principal Component Analysis (PCA) in the framework of the MoM principle. The proposal is not only computationally efficient but also theoretically appealing. It is well known that the theoretical understanding of many classical Empirical Risk Minimization (ERM) [22] such as PCA hinges on the assumptions that the data should be independently and identically distributed (i.i.d.) and have sub-gaussian behavior. However, real data that may be corrupted with outliers do not offer us the luxury to make such simplifying assumptions. Towards our theoretical investigation, we assume that the dataset can be split into two categories: the set of inliers (\mathcal{I}) and the set of outliers (\mathcal{O}), i.e., $\{1, \dots, N\} = \mathcal{I} \cup \mathcal{O}$. The data points in \mathcal{I} are assumed to be independently distributed according to the distribution P , which has a finite fourth moment. We make no assumptions on the points in \mathcal{O} ; thus, allowing them to be dependent, unboundedly large, having distributions that are entirely dissimilar to P , allowing them to be heavy-tailed, etc. Our theoretical analysis hinges on the application of Rademacher complexity [37], and symmetrization arguments [22, 38]. From a theoretical viewpoint, we emphasize that our analyses are derived under more general and interpretable conditions compared to the literature [39]. To further generalize the

proposed setup, we conduct all our theoretical analyses in a separable Hilbert space. This allows us to derive *dimension-free bounds* that only depend on the data distribution through the fourth moment of the inliers. We quickly recover the data results in a finite-dimensional vector space showing that the derived rates match the state-of-the-art [24, 34].

The main contributions of this article can be summarized as follows:

- This paper proposes a simple yet efficient framework for robust PCA under the median of means paradigm. Apart from being practically efficient, the method comes with a strong theoretical backbone of finite-sample error rates under the mild assumption of the existence of a finite fourth moment of the underlying data distribution. Such consistency guarantees and error rates that are derived subsequently, ensure that the results are reliable and accurate under mild assumptions.
- Furthermore, the derived generalization bounds are dimension-free meaning that the error rate is also valid for infinite-dimensional Hilbert spaces.
- We emphasize that as opposed to many prominent works [7, 40], we only assume that the number of outliers is $o(N)$, which is the natural definition of outliers. We do not make any assumptions on the distribution of the outliers allowing them to be dependent, unboundedly large, having distributions that are entirely dissimilar to the inlier distribution, etc.
- The detailed experimental analysis via simulation and real-life datasets on background modeling in video and anomaly detection demonstrates the efficacy of MoMPCA compared to the state-of-the-art in different experimental settings, indicating that the the proposed method is highly effective in practice.

The rest of the paper is organized as follows. In section 2, we formulate the MoMPCA, followed by a detailed theoretical analysis under minimal and interpretable assumptions in section 3. The experimental results are discussed in section 4, followed by concluding remarks in section 5.

Notations: Before we proceed further, we discuss a few notations used in this paper. Vectors are denoted with bold lower-case letters, and matrices are denoted with bold uppercase letters. $\langle \mathbf{A}, \mathbf{B} \rangle = \text{trace}(\mathbf{A}^\top \mathbf{B})$ denotes the Frobenious inner product between two matrices. $\|\mathbf{A}\| = \sqrt{\langle \mathbf{A}, \mathbf{A} \rangle}$ denotes the Frobenious norm of the matrix \mathbf{A} . $\mathbb{P}(E)$ denotes the probability of the event E and $\mathbb{E}_{\mathbf{Z}}(\cdot)$ denotes the expectation with respect to the random vector \mathbf{Z} . A random variable σ is said to be Rademacher if it takes values in $\{+1, -1\}$ with equal probability. $[N]$ denotes the set $\{1, \dots, N\}$, for any $N \geq 0$ and 2^A denotes the power set of the A . For any two sets A and B , A^B denotes the set of all functions from B to A . $\mu_k = \int \|\mathbf{x}\|_2^k dP$ denote the k -th moment of P . \mathcal{Q}_d denotes the set of all $p \times p$ real projection matrices of rank d . $one(\cdot)$ denotes the indicator function.

1.1 Related Works

This section discusses some of the works related to robust clustering. The most noted work in this direction is arguably the work by [7], which appeals to the philosophy of writing the data matrix as a sum of a low rank and a sparse matrix and minimizing the subsequent approximation error. [15] extended this idea by developing a convex program for a low-rank and block-sparse matrix decomposition. A survey on these papers can be found in [16]. [41] developed a new subspace selection method called angle linear discriminant embedding (ALDE) for dimensionality reduction in a supervised learning setting. Angle PCA proposed by [17] develops an iterative algorithm to minimize an ℓ_2 norm-based error and maximize the summation of the ratio between the variance

and the reconstruction error to preserve rotational invariance while tackling outliers. [42] further extended these ideas to develop angular embedding for conducting robust PCA. [43, 44] introduced Grassman averages to express dimensionality reduction as an average of the subspaces spanned by the data. The authors further exploit its properties to develop a robust Grassman average as a form of robust PCA. [45] showed the application of robust PCA in image and video processing. Other than the median of the means PCA method, there are other types of robust PCA methods as well, such as the optimal mean methods [46, 47] and the avoid mean calculation [48]. There has also been an array of work based on geometric median-based approaches [18, 19, 20, 21], which focuses on a robust estimation of the covariance matrix and finding the eigendecomposition of the same to find the proper subspace to project.

1.2 Motivation and a Proof of Concept Result

Robust PCA is commonly formulated by assuming that the data matrix can be decomposed into a low-rank signal component and a noise component. However, this framework is limited by the assumption that the effect of outliers is mild and cannot grow unboundedly large. To address this issue, the authors propose using the median of means framework, which is commonly used in robust mean estimation, to view traditional PCA as an empirical risk minimization problem. Because the objective cannot be solved using the eigen-decomposition trick, the authors propose an alternative method called projected Adagrad. The authors note that the most challenging aspect of the project was extending the theoretical results to an infinite-dimensional Hilbert space and deriving dimension-free bounds under only the existence of a finite fourth moment of the data distribution. This result not only provides meaningful conclusions with minimal assumptions but also paves the way for future research on robust kernel-based methods.

As a motivating example, in Fig. 1, we show the results of classical PCA and MoMPCA on a toy dataset (available at <https://github.com/SaptarshiC98/MOMPCHA>). The dataset has 1000 observations, out of which 10 of them, i.e., 1% are outliers. The inliers are generated from a 2-dimensional Gaussian random variable with variance 10 in the first dimension, 1 in the second dimension, and covariance 8. The outliers are generated from another 2-dimensional Gaussian random variable with mean vector (15, 50), variance 5 in each dimension with zero covariance between them. Finally, we run the vanilla PCA (shown in red) and the proposed MoMPCA (shown in blue) and plot their first principal components. From Fig. 1, it is clear that a mere 1% outlying observations are enough to render the vanilla PCA ineffective, whereas, MoMPCA correctly identifies the direction of maximum variation. In terms of excess risk (details provided in section 4.1), we calculate that the excess risk for vanilla PCA is 20.6850 where, in comparison, the extra risk for MoMPCA is only 0.3104, proving its efficacy.

2 PCA with Median of Means

2.1 Problem Setup

We will follow the same notations as described in section 1. One should note that the PCA objective function (1) can be written as $\int \xi_V(\mathbf{x}) P_N(d\mathbf{x}) = \frac{1}{n} \sum_{i=1}^N \xi_V(\mathbf{x}_i)$, with $\xi_V(\mathbf{x}) = \mathbf{x}^\top (\mathbf{I} - \mathbf{Q})\mathbf{x}$. Here $P_N = \frac{1}{N} \sum_{i=1}^N \delta_{\mathbf{x}_i}$ denotes the empirical measure, based on \mathcal{X} , i.e. $P_N(A) = \frac{1}{n} \sum_{i=1}^n \mathbb{1}\{\mathbf{x}_i \in A\}$, for any set A .

MoM does not directly minimize the empirical risk (1). Instead, it starts with a partitioning of the data into L groups B_1, \dots, B_L (i.e. $B_\ell \in 2^{[n]}$, $\cup_{\ell=1}^L B_\ell = [n]$ and $B_\ell \cap B_{\ell'} = \emptyset$ for $\ell \neq \ell'$), each of which contains exactly B many elements (repudiating a few observations when L does not

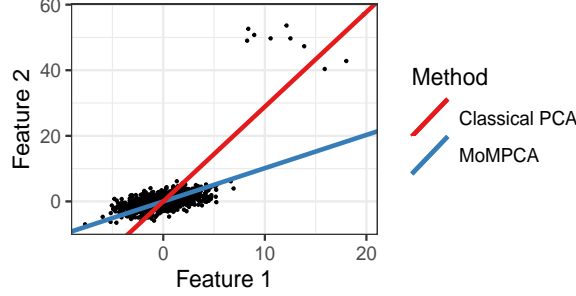


Figure 1: The first principal component found out by PCA and MoM PCA for the motivating example. Even in the presence of only 1% outlying observations, the classical PCA can render spurious results while MoM PCA finds the direction of maximum variation efficiently.

divide n). One can make a uniform at random assignment of the partitions or shuffle them *on the run* [35]. Let P_{B_ℓ} denote the empirical distribution of $\{\mathbf{x}_i\}_{i \in B_\ell}$. For notational simplicity, we write, $\mu f = \int f d\mu$. We formulate the **Median of Means Principal Components Analysis** (MoMPCA) as the solution to the minimization problem of the following objective function,

$$\text{MoM}_L^N(\xi_V) = \text{Median}(\{P_{B_\ell} \xi_V : \ell = 1, \dots, L\}) = \frac{1}{B} \text{Median} \left(\sum_{i \in B_1} \xi_V(\mathbf{x}_i), \dots, \sum_{i \in B_L} \xi_V(\mathbf{x}_i) \right) \quad (2)$$

subject to $V \in \mathcal{V}_d$. A pictorial representation of objective 2 is given in Fig. 2. Compared to their ERM counterparts, MoM estimators appear to exhibit stronger robustness as under mild assumptions, the outliers can affect only a subset of the partitions while the others remain free of outliers. Taking the median over partitions negates the effect of such contrived partitions, thus neutralizing the influence of outliers. Works like [49, 50] formally analyzes the robustness of the MoM estimators through breakdown points.

2.2 Optimization

Optimizing (2) is tractable via gradient-based methods. It is easy to see that we can write $\mathbf{Q} = \mathbf{V}\mathbf{V}^\top$, where \mathbf{V} is a $p \times d$ real column-orthonormal matrix. Thus, making a variable transform, we can write, (2) as

$$\text{MoM}_L^N(g_V) = \frac{1}{B} \text{Median} \left(\sum_{i \in B_1} g_V(\mathbf{x}_i), \dots, \sum_{i \in B_L} g_V(\mathbf{x}_i) \right) \quad (3)$$

where $g_V(\mathbf{x}) = \mathbf{x}^\top (I - \mathbf{V}\mathbf{V}^\top) \mathbf{x}$. At the t -th iteration, let the median partition be $\ell_{\text{med}}^{(t)}$, i.e. $\ell_t \in [L]$ be such that $\text{MoM}_L^N(g_{\mathbf{V}^{(t)}}) = \frac{1}{B} \sum_{i \in B_{\ell_t}} g_{\mathbf{V}^{(t)}}(\mathbf{x}_i)$. According to [24], $\nabla \text{MoM}_L^N(g_{\mathbf{V}^{(t)}}) = \frac{2}{B} \sum_{i \in B_{\ell_{\text{med}}^{(t)}}} \mathbf{x}_i \mathbf{x}_i^\top \mathbf{V}^{(t)}$. However, after taking a gradient step, $\mathbf{V}^{(t)} - \eta \frac{1}{B} \sum_{i \in B_{\ell_{\text{med}}^{(t)}}} \mathbf{x}_i \mathbf{x}_i^\top \mathbf{V}^{(t)}$, the resultant matrix may not be column orthonormal. Following [51], we apply a Gram-Schmidt algorithm to make the columns of this resultant matrix orthonormal. Let $\mathcal{P}_{\text{orth}}(\mathbf{V})$ denote the resultant matrix after orthonormalizing the columns of \mathbf{V} . One can thus use the following gradient descent update:

$$\mathbf{V}^{(t+1)} \leftarrow \mathcal{P}_{\text{orth}} \left(\mathbf{V}^{(t)} - \eta \frac{1}{B} \sum_{i \in B_{\ell_{\text{med}}^{(t)}}} \mathbf{x}_i \mathbf{x}_i^\top \mathbf{V}^{(t)} \right).$$

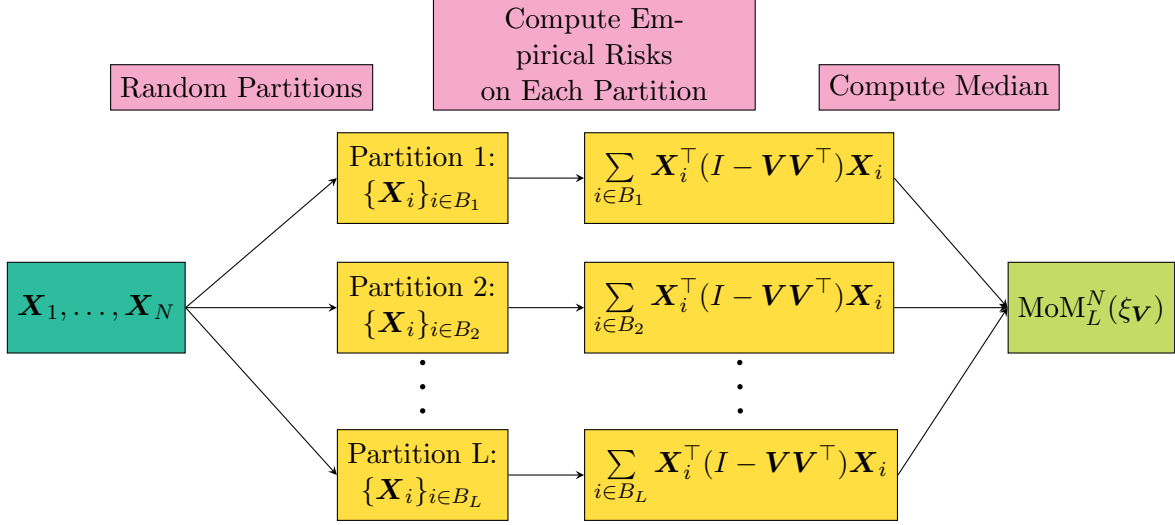


Figure 2: A pictorial illustration of median-of-means PCA objective.

Algorithm 1 gives a formal description of the proposed gradient descent updates to optimize (2).

2.3 Centering

One should note that the aforementioned formulation is for centered observations. If the data is not centered, one must first center the observations by subtracting a robust estimate of location from each point. This is to emphasize that under outlier contamination, the sample mean may not be a reasonable estimate for the measure of central tendency for the data, and one has to resort to other robust estimates of the location, such as component-wise median or data depth based measures, to center the data.

2.4 Time Complexity

It is a well known fact that in a dataset with n number of datapoints and p many features, the time complexity of vanilla PCA is $\mathcal{O}(\min\{n^3, p^3\})$. For our method, we note that, the computation of v_ℓ 's require $\mathcal{O}(kp^2(p \vee b))$ time. This is because, $v_\ell = \text{trace}(\mathbf{V}^{(t)}(\mathbf{V}^{(t)})^\top \sum_{i \in B_\ell} \mathbf{x}_i \mathbf{x}_i^\top)$ and requires $\mathcal{O}(p^2b + p^2d + p^3 + p) = \mathcal{O}(p^2(b \vee p))$, taking into account all the matrix multiplications and trace computation. The median computation takes $\mathcal{O}(L)$ time. For the computation of $\mathbf{V}^{(t+1)}$, we note that, the gradient computation takes $\mathcal{O}(bp^2 + p^2d + p^2) = \mathcal{O}(p^2b)$ time and the Gram-Schmidt orthogonalization takes $\mathcal{O}(pd^2)$ time, making a total of $\mathcal{O}(p^2b + pd^2)$ time. Thus the per iteration complexity of the loop is $\mathcal{O}(p^2(b \vee p) + p^2b + pd^2 + L)$ time. In general, $b > p$ and the per iteration complexity becomes $\mathcal{O}(p^2b + pd^2 + L)$.

3 Theoretical Properties

3.1 Notation and Setup

Instead of performing the analysis on a real vector space as was done in our recent MoM-based robust clustering work [34], here we develop our proofs for a (real) Hilbert space in context to robust PCA. Suppose the data is observed in a real separable Hilbert space \mathcal{H} , i.e., $\{X_i\}_{i \in [n]} \subset \mathcal{H}$. Let the norm in \mathcal{H} be denoted by $\|\cdot\|$. A linear operator $L : \mathcal{H} \rightarrow \mathcal{H}$, is said to be Hilbert-Schmidt if

Algorithm 1 Median of Means Principal Component Analysis (MoMPCA)

Input: The dataset $\mathcal{X} = \{\mathbf{x}_1, \dots, \mathbf{x}_n\}$, L , d , η .

Output: $\widehat{\mathbf{Q}}_{N,L}$.

Initialization: Randomly partition $[N]$ into L many partitions of equal length.

Compute the feature-wise median $\boldsymbol{\mu}$ of \mathcal{X} . Replace \mathbf{x}_i by $\mathbf{x}_i - \boldsymbol{\mu}$.

Compute the first d eigenvectors of $\sum_{i=1}^n \mathbf{x}_i \mathbf{x}_i^\top$ and stack them as columns of $\mathbf{V}^{(0)}$.

repeat

 Compute $v_\ell \leftarrow \sum_{i \in B_\ell} \mathbf{x}_i^\top (I - \mathbf{V}^{(t)} (\mathbf{V}^{(t)})^\top) \mathbf{x}_i$

 Compute the median class ℓ_{med} , such that $v_{\ell_{\text{med}}} = \text{median}(\{v_\ell\}_{\ell=1}^L)$

$$\mathbf{V}^{(t+1)} \leftarrow \mathcal{P}_{\text{orth}} \left(\mathbf{V}^{(t)} - \frac{\eta}{B} \sum_{i \in B_{\ell_{\text{med}}^{(t)}}} \mathbf{x}_i \mathbf{x}_i^\top \mathbf{V}^{(t)} \right).$$

until objective $\mathbf{V}^{(t)}$ converges

Compute $\widehat{\mathbf{Q}}_{N,L} \leftarrow \mathbf{V}^{(t)} (\mathbf{V}^{(t)})^\top$.

$\sum_{i \geq 1} \|L e_i\|^2 < \infty$ and the sum is independent of the chosen orthonormal basis $\{e_i\}_{i \geq 1}$ (of \mathcal{H}). Let $HS(\mathcal{H})$ be the set of all Hilbert-Schmidt linear operators. An inner product on $HS(\mathcal{H})$ is defined as, $\langle L_1, L_2 \rangle = \sum_{i \geq 1} \langle L_1 e_i, L_2 e_i \rangle$. It can be shown that $HS(\mathcal{H})$ is also a separable (real) Hilbert space. The trace of a linear operator is defined as $\text{tr}(L) = \sum_{i \geq 1} \langle L e_i, e_i \rangle$.

For any $x, y \in \mathcal{H} \setminus \{0\}$, the outer product operator $x \otimes y$ is defined as $(x \otimes y)(z) = \langle y, z \rangle x$. This outer product satisfies the following properties.

- $\|x \otimes y\|_{HS(\mathcal{H})} = \|x\| \|y\|$.
- $\text{tr}(x \otimes y) = \langle x, y \rangle$.
- $\langle L, x \otimes y \rangle_{HS(\mathcal{H})} = \langle L y, x \rangle$

Recall that if U is an orthogonal projector operator in \mathcal{H} , then $U^2 = U$. Moreover, $\|Ux\|^2 = \langle x, Ux \rangle \leq \|x\|^2$ and $\langle x \otimes y, U \rangle_{HS(\mathcal{H})} = \langle Ux, Uy \rangle$. U has rank $d < \infty$, iff it is Hilbert-Schmidt and

$$\|U\|_{HS(\mathcal{H})}^2 = d; \quad \text{tr}(U) = d.$$

Suppose V is a closed subspace of \mathcal{H} , then Π_V denotes the (unique) orthogonal projector onto V . V^\perp represents the orthogonal complement of V .

We aim to find the “best” subspace of dimension d in this Hilbert space that minimizes the reconstruction error. Hence we consider the following objective, similar to equation 2

We assume that the dataset can be split into two categories: the set of inliers (\mathcal{I}) and the set of outliers (\mathcal{O}), i.e., $[N] = \mathcal{I} \cup \mathcal{O}$. We will assume the following in the data generation process.

A1. $\{\mathbf{x}_i\}_{i \in \mathcal{I}}$ are independently and identically distributed (i.i.d) according to the distribution P .

A2. $\mathbb{E}_{\mathbf{x} \sim P}(\mathbf{x}) = \mathbf{0}$ and $\mu_4 = \mathbb{E}_{X \sim P} \|\mathbf{x}\|^4 < \infty$.

A3. $\exists \eta > 0$, such that $L > (2 + \eta)|\mathcal{O}|$.

We emphasize that we do not make any assumptions about the distributions of the outlying observations. They are even allowed to be dependent and may even come from some heavy-tailed distributions. Assumptions A1 and A2 state that the inlying observations are independently and

identically generated from some distribution with zero mean and a finite fourth moment. To see the significance of assumption A3, one should note that by the pigeonhole principle, (strictly) less than half of the partitions may contain an outlying observation. More than half of the partitions, thus, do not contain an outlier. Since the median is driven by the majority half of the partitions, naturally by A3, since the median is only affected by the objective function value of the majority half of these partitions, the MoM estimates can be expected only to be based on the inlying observations. We note that our analysis does not require “ $L > 4|\mathcal{O}|$ ” as in [39] but only requires that $L > (2 + \eta)|\mathcal{O}|$, which is a much weaker condition. Moreover, opposed to [39], A3 has nice practical interpretations.

Let

$$\xi_V(\mathbf{x}) = \|\mathbf{x} - \mathbf{\Pi}_V \mathbf{x}\|^2 = \|\mathbf{\Pi}_{V^\perp} \mathbf{x}\|^2 = \langle \mathbf{\Pi}_{V^\perp} \mathbf{x}, \mathbf{\Pi}_{V^\perp} \mathbf{x} \rangle = \langle \mathbf{\Pi}_{V^\perp}, \mathbf{x} \otimes \mathbf{x} \rangle_{HS(\mathcal{H})}.$$

For notational simplicity, for any function g , We define the operator, $\text{MoM}_L^N(\cdot)$ as follows:

$$\text{MoM}_L^N(g) = \frac{1}{B} \text{Median} \left(\sum_{i \in B_1} g(\mathbf{x}_i), \dots, \sum_{i \in B_L} g(\mathbf{x}_i) \right).$$

It is easy to observe that the MoMPCA problem in section 2 can be restated as,

$$\min_{V \in \mathcal{V}_d} \text{MoM}_L^N(\xi_V).$$

Here, \mathcal{V}_d denotes the set of all d -dimensional subspaces of \mathcal{H} . Let the unique minimizer to the above problem be $\hat{V}_d = \text{argmin}_{V \in \mathcal{V}_d} \text{MoM}_L^N(\xi_V)$. Let $V_d^* = \text{argmin}_{V \in \mathcal{V}_d} P\xi_V$ be the global population minimizer. The excess risk of the estimate, \hat{V}_d is given by,

$$\mathfrak{R}(\hat{V}_d) = P\xi_{\hat{V}_d} - P\xi_{V_d^*} = \int \xi_{\hat{V}_d} dP - \inf_{V \in \mathcal{V}_d} \int \xi_V dP \quad (4)$$

We note that $P\xi_{V_d^*} \leq P\xi_V$ and $\text{MoM}_L^N(\xi_{\hat{V}_d}) \leq \text{MoM}_L^N(\xi_V)$, for all $V \in \mathcal{V}_d$. Thus,

$$\begin{aligned} |P\xi_{\hat{V}_d} - P\xi_{V_d^*}| &= P\xi_{\hat{V}_d} - P\xi_{V_d^*} \\ &= (P\xi_{\hat{V}_d} - \text{MoM}_L^N(\xi_{\hat{V}_d})) + (\text{MoM}_L^N(\xi_{\hat{V}_d}) \\ &\quad - \text{MoM}_L^N(\xi_{V_d^*}) + (\text{MoM}_L^N(\xi_{V_d^*}) - P\xi_{V_d^*})) \\ &\leq (P\xi_{\hat{V}_d} - \text{MoM}_L^N(\xi_{\hat{V}_d})) + (\text{MoM}_L^N(\xi_{V_d^*}) - P\xi_{V_d^*}) \\ &\leq 2 \sup_{V \in \mathcal{V}_d} |\text{MoM}_L^N(\xi_V) - P\xi_V|. \end{aligned} \quad (5)$$

It is thus, enough to prove bounds on the uniform deviation $\sup_{V \in \mathcal{V}_d} |\text{MoM}_L^N(\xi_V) - P\xi_V|$. Towards that, we will first derive bounds on the Rademacher complexity in the following section, followed by our main results.

3.2 Bounds on the Rademacher Complexity

For our theoretical understanding of MoMPCA, we need to compute the Rademacher complexity of the function class $\Xi_d = \{\xi_V : V \in \mathcal{V}_d\}$. We first recall the definition of Rademacher complexity. Let $\mathbf{y}_1, \dots, \mathbf{y}_m \stackrel{i.i.d.}{\sim} P$ be random variables in some space \mathcal{S} . Suppose $\mathcal{F} \subseteq \mathbb{R}^{\mathcal{S}}$ be a class of functions

from \mathcal{S} to \mathbb{R} and let $\sigma_1, \dots, \sigma_m$ be i.i.d. Rademacher random variables. The empirical Rademacher complexity, based on $\mathcal{Y} = \{\mathbf{y}_1, \dots, \mathbf{y}_m\}$ is defined as:

$$\hat{R}_{\mathcal{Y}}(\mathcal{F}) = \frac{1}{m} \mathbb{E} \left(\sup_{f \in \mathcal{F}} \sum_{i=1}^m \sigma_i f(\mathbf{y}_i) \middle| \mathcal{Y} \right).$$

Similarly, the population Rademacher complexity is defined as

$$R_m(\mathcal{F}) = \mathbb{E}(R_{\mathcal{Y}}(\mathcal{F})) = \frac{1}{m} \mathbb{E} \sup_{f \in \mathcal{F}} \sum_{i=1}^m \sigma_i f(\mathbf{y}_i).$$

We now compute the Rademacher complexity of the function class $\{\xi_V : V \in \mathcal{V}_d\}$ in Theorem 1.

Theorem 1. Suppose $\Xi_d = \{\xi_V : V \in \mathcal{V}_d\}$. Let $\mathbf{y}_1, \dots, \mathbf{y}_m \stackrel{i.i.d.}{\sim} P$, with P satisfying Assumption 2. Then, $R_m(\Xi_d) \leq \sqrt{\frac{d\mu_4}{m}}$.

Proof. Suppose $\mathbf{y}_1, \dots, \mathbf{y}_m \stackrel{i.i.d.}{\sim} P$ and let $\mathcal{Y} = \{\mathbf{y}_1, \dots, \mathbf{y}_m\}$. The empirical Rademacher complexity is thus, given by,

$$\begin{aligned} \hat{R}_{\Xi_d}(Q) &= \frac{1}{m} \mathbb{E}_{\boldsymbol{\sigma}} \sup_{V \in \mathcal{V}_d} \sum_{i=1}^m \sigma_i \xi_V(\mathbf{y}_i) \\ &= \frac{1}{m} \mathbb{E}_{\boldsymbol{\sigma}} \sup_{V \in \mathcal{V}_d} \sum_{i=1}^m \sigma_i (\|\mathbf{y}_i\|_2^2 - \langle \mathbf{\Pi}_V, \mathbf{y}_i \otimes \mathbf{y}_i \rangle_{HS(\mathcal{H})}) \\ &= \frac{1}{m} \mathbb{E}_{\boldsymbol{\sigma}} \sup_{V \in \mathcal{V}_d} \left\langle \mathbf{\Pi}_V, \sum_{i=1}^m \sigma_i \mathbf{y}_i \otimes \mathbf{y}_i \right\rangle_{HS(\mathcal{H})} \\ &\leq \frac{1}{m} \mathbb{E}_{\boldsymbol{\sigma}} \sup_{V \in \mathcal{V}_d} \|\mathbf{\Pi}_V\|_{HS(\mathcal{H})} \left\| \sum_{i=1}^m \sigma_i \mathbf{y}_i \otimes \mathbf{y}_i \right\|_{HS(\mathcal{H})} \end{aligned} \tag{6}$$

$$\begin{aligned} &\leq \frac{\sqrt{d}}{m} \mathbb{E}_{\boldsymbol{\sigma}} \left\| \sum_{i=1}^m \sigma_i \mathbf{y}_i \otimes \mathbf{y}_i \right\|_{HS(\mathcal{H})} \\ &\leq \frac{\sqrt{d}}{m} \sqrt{\mathbb{E}_{\boldsymbol{\sigma}} \left\| \sum_{i=1}^m \sigma_i \mathbf{y}_i \otimes \mathbf{y}_i \right\|_{HS(\mathcal{H})}^2} \\ &= \frac{\sqrt{d}}{m} \sqrt{\sum_{i=1}^m \|\mathbf{y}_i \otimes \mathbf{y}_i\|_{HS(\mathcal{H})}^2} \\ &= \frac{\sqrt{d}}{m} \sqrt{\sum_{i=1}^m \|\mathbf{y}_i\|^4} \end{aligned} \tag{7}$$

Here, inequalities (6) and (7) follow from appealing to Cauchy-Schwartz and Jensens's inequalities, respectively. Thus,

$$R_m(\Xi_d) = \mathbb{E}_{\mathcal{Y}} \hat{R}_{\mathcal{X}}(\Xi_d)$$

$$\begin{aligned}
&= \frac{1}{m} \sqrt{d} \mathbb{E} \left[\sqrt{\sum_{i=1}^m \|\mathbf{y}_i\|^4} \right] \\
&\leq \frac{1}{m} \sqrt{d} \sqrt{\sum_{i=1}^m \mathbb{E} \|\mathbf{y}_i\|^4} \\
&= \sqrt{\frac{d\mu_4}{m}}.
\end{aligned} \tag{8}$$

Inequality (8) follows from Jensen's inequality. \square

3.3 Uniform Concentration Bounds

We are now ready to state and prove the uniform concentration bound result in Theorem 2. Theorem 2 asserts that with a high probability, $\sup_{V \in \mathcal{V}_d} |\text{MoM}_L^N(\xi_V) - P\xi_V| \lesssim \sqrt{\frac{L}{N}} + \frac{\sqrt{|\mathcal{I}|}}{N}$ with a very high probability.

Theorem 2. *Under A1–3, and $N > L$, with probability at least, $1 - 2e^{-2L\left(\frac{2}{4+\eta} - \frac{|\mathcal{O}|}{L}\right)^2}$,*

$$\sup_{V \in \mathcal{V}_d} |\text{MoM}_L^N(\xi_V) - P\xi_V| \leq C \sqrt{\mathbb{E} \|\mathbf{x}\|^4} \left(\sqrt{\frac{L}{N}} + \frac{\sqrt{d|\mathcal{I}|}}{N} \right),$$

$$\text{with } C = 2 \max \left\{ \sqrt{\frac{8(4+\eta)}{\eta}}, \frac{16(4+\eta)}{\eta} \right\}.$$

Proof. Suppose $\epsilon > 0$. We will first bound the probability of $\sup_{V \in \mathcal{V}_d} |\text{MoM}_L^N(\xi_V) - P\xi_V| > \epsilon$. To do so, we will individually bound the probabilities of the events, $\sup_{V \in \mathcal{V}_d} (\text{MoM}_L^N(\xi_V) - P\xi_V) > \epsilon$ and $\sup_{V \in \mathcal{V}_d} (P\xi_V - \text{MoM}_L^N(\xi_V)) > \epsilon$. We note that if $\sup_{V \in \mathcal{V}_d} \sum_{\ell=1}^L \mathbb{1}\{(P - P_{B_\ell})\xi_V > \epsilon\} > \frac{L}{2}$, then, $\sup_{V \in \mathcal{V}_d} (P\xi_V - \text{MoM}_L^N(\xi_V)) > \epsilon$. Here $\mathbb{1}\{\cdot\}$ denote the indicator function. Let $\varphi(t) = (t-1)\mathbb{1}\{1 \leq t \leq 2\} + \mathbb{1}\{t > 2\}$. Clearly,

$$\mathbb{1}\{t \geq 2\} \leq \varphi(t) \leq \mathbb{1}\{t \geq 1\}. \tag{9}$$

We observe that,

$$\begin{aligned}
&\sup_{V \in \mathcal{V}_d} \sum_{\ell=1}^L \mathbb{1}\{(P - P_{B_\ell})\xi_V > \epsilon\} \\
&\leq \sup_{V \in \mathcal{V}_d} \sum_{\ell \in \mathcal{L}} \mathbb{1}\{(P - P_{B_\ell})\xi_V > \epsilon\} + |\mathcal{O}| \\
&\leq \sup_{V \in \mathcal{V}_d} \sum_{\ell \in \mathcal{L}} \varphi \left(\frac{2(P - P_{B_\ell})\xi_V}{\epsilon} \right) + |\mathcal{O}| \\
&\leq \sup_{V \in \mathcal{V}_d} \sum_{\ell \in \mathcal{L}} \mathbb{E} \varphi \left(\frac{2(P - P_{B_\ell})\xi_V}{\epsilon} \right) + |\mathcal{O}| + \sup_{V \in \mathcal{V}_d} \sum_{\ell \in \mathcal{L}} \left[\varphi \left(\frac{2(P - P_{B_\ell})\xi_V}{\epsilon} \right) - \mathbb{E} \varphi \left(\frac{2(P - P_{B_\ell})\xi_V}{\epsilon} \right) \right].
\end{aligned} \tag{10}$$

To bound $\sup_{V \in \mathcal{V}_d} \sum_{\ell=1}^L \mathbb{1}\{(P - P_{B_\ell})\xi_V > \epsilon\}$, we will first bound the quantity, $\mathbb{E} \varphi \left(\frac{2(P - P_{B_\ell})\xi_V}{\epsilon} \right)$. We observe that,

$$\mathbb{E} \varphi \left(\frac{2(P - P_{B_\ell})\xi_V}{\epsilon} \right) \leq \mathbb{E} \left[\mathbb{1} \left\{ \frac{2(P - P_{B_\ell})\xi_V}{\epsilon} > 1 \right\} \right]$$

$$\begin{aligned}
&= \mathbb{P} \left[(P - P_{B_\ell}) \xi_V > \frac{\epsilon}{2} \right] \\
&\leq \frac{4}{\epsilon^2} \text{Var}((P - P_{B_\ell}) \xi_V) \\
&= \frac{4}{\epsilon^2} \text{Var}(P_{B_\ell} \xi_V) \\
&= \frac{4}{B\epsilon^2} \text{Var}(\|\mathbf{\Pi}_{V^\perp} \mathbf{x}\|^2) \\
&\leq \frac{4}{B\epsilon^2} \mathbb{E} \|\mathbf{\Pi}_{V^\perp} \mathbf{x}\|^4 \\
&\leq \frac{4}{B\epsilon^2} \mathbb{E} \|\mathbf{x}\|^4
\end{aligned} \tag{11}$$

Here equation (11) follows from Chebyshev's inequality. We now concentrate on bounding the term $\sup_{V \in \mathcal{V}_d} \sum_{\ell \in \mathcal{L}} \left[\varphi \left(\frac{2(P - P_{B_\ell}) \xi_V}{\epsilon} \right) - \mathbb{E} \varphi \left(\frac{2(P - P_{B_\ell}) \xi_V}{\epsilon} \right) \right]$. Appealing to Theorem 26.5 of [52] we observe that, with probability at least $1 - e^{-2L\delta^2}$, $\forall V \in \mathcal{V}_d$,

$$\frac{1}{L} \sum_{\ell \in \mathcal{L}} \varphi \left(\frac{2(P - P_{B_\ell}) \xi_V}{\epsilon} \right) \leq \mathbb{E} \left[\frac{1}{L} \sum_{\ell \in \mathcal{L}} \varphi \left(\frac{2(P - P_{B_\ell}) \xi_V}{\epsilon} \right) \right] + 2\mathbb{E} \left[\sup_{V \in \mathcal{V}_d} \frac{1}{L} \sum_{\ell \in \mathcal{L}} \sigma_\ell \varphi \left(\frac{2(P - P_{B_\ell}) \xi_V}{\epsilon} \right) \right] + \delta. \tag{12}$$

Here $\{\sigma_\ell\}_{\ell \in \mathcal{L}}$ are independent Rademacher variables. Suppose that $\{\xi_i\}_{i=1}^n$ are independent Rademacher random variables and independent of $\{\sigma_\ell\}_{\ell \in \mathcal{L}}$. From equation (12), we get,

$$\begin{aligned}
&\frac{1}{L} \sup_{V \in \mathcal{V}_d} \sum_{\ell \in \mathcal{L}} \left[\varphi \left(\frac{2(P - P_{B_\ell}) \xi_V}{\epsilon} \right) - \mathbb{E} \varphi \left(\frac{2(P - P_{B_\ell}) \xi_V}{\epsilon} \right) \right] \\
&\leq 2\mathbb{E} \left[\sup_{V \in \mathcal{V}_d} \frac{1}{L} \sum_{\ell \in \mathcal{L}} \sigma_\ell \varphi \left(\frac{2(P - P_{B_\ell}) \xi_V}{\epsilon} \right) \right] + \delta \\
&\leq \frac{4}{L\epsilon} \mathbb{E} \left[\sup_{V \in \mathcal{V}_d} \sum_{\ell \in \mathcal{L}} \sigma_\ell (P - P_{B_\ell}) \xi_V \right] + \delta.
\end{aligned} \tag{13}$$

Equation (13) follows from the fact that $\varphi(\cdot)$ is 1-Lipschitz and appealing to Lemma 26.9 of [52]. We now introduce a phantom sample $\mathcal{X}' = \{\mathbf{x}'_1, \dots, \mathbf{x}'_n\}$, which are i.i.d. and follows the law P , independent of \mathcal{X} . Thus, equation (13) further equals the following quantity.

$$\begin{aligned}
&= \frac{4}{L\epsilon} \mathbb{E} \left[\sup_{V \in \mathcal{V}_d} \sum_{\ell \in \mathcal{L}} \sigma_\ell \mathbb{E}_{\mathcal{X}'}((P'_{B_\ell} - P_{B_\ell}) \xi_V) \right] + \delta \\
&\leq \frac{4}{L\epsilon} \mathbb{E} \left[\sup_{V \in \mathcal{V}_d} \sum_{\ell \in \mathcal{L}} \sigma_\ell (P'_{B_\ell} - P_{B_\ell}) \xi_V \right] + \delta \\
&= \frac{4}{L\epsilon} \mathbb{E} \left[\sup_{V \in \mathcal{V}_d} \sum_{\ell \in \mathcal{L}} \sigma_\ell \frac{1}{B} \sum_{i \in B_\ell} (\xi_V(\mathbf{x}'_i) - \xi_V(\mathbf{x}_i)) \right] + \delta \\
&= \frac{4}{BL\epsilon} \mathbb{E} \left[\sup_{V \in \mathcal{V}_d} \sum_{\ell \in \mathcal{L}} \sigma_\ell \sum_{i \in B_\ell} \xi_i (\xi_V(\mathbf{x}'_i) - \xi_V(\mathbf{x}_i)) \right] + \delta
\end{aligned} \tag{14}$$

$$\begin{aligned}
&= \frac{4}{N\epsilon} \mathbb{E} \left[\sup_{V \in \mathcal{V}_d} \sum_{\ell \in \mathcal{L}} \sum_{i \in B_\ell} \sigma_\ell \xi_i (\xi_V(\mathbf{x}'_i) - \xi_V(\mathbf{x}_i)) \right] + \delta \\
&\leq \frac{4}{N\epsilon} \mathbb{E} \left[\sup_{V \in \mathcal{V}_d} \sum_{\ell \in \mathcal{L}} \sum_{i \in B_\ell} \sigma_\ell \xi_i (\xi_V(\mathbf{x}'_i) + \xi_V(\mathbf{x}_i)) \right] + \delta \\
&= \frac{4}{N\epsilon} \mathbb{E} \left[\sup_{V \in \mathcal{V}_d} \sum_{i \in \mathcal{J}} \gamma_i (\xi_V(\mathbf{x}'_i) + \xi_V(\mathbf{x}_i)) \right] \tag{15}
\end{aligned}$$

$$= \frac{8}{N\epsilon} \mathbb{E} \left[\sup_{V \in \mathcal{V}_d} \sum_{i \in \mathcal{J}} \gamma_i \xi_V(\mathbf{x}_i) \right] + \delta \tag{16}$$

$$\begin{aligned}
&\leq \frac{8}{N\epsilon} \sqrt{d\mu_4 |\mathcal{J}|} + \delta \\
&\leq \frac{8}{N\epsilon} \sqrt{d\mu_4 |\mathcal{I}|} + \delta. \tag{17}
\end{aligned}$$

Equation (14) follows from observing that $(\xi_V(\mathbf{x}'_i) - \xi_V(\mathbf{x}_i)) \stackrel{d}{=} \xi_i(\xi_V(\mathbf{x}'_i) - \xi_V(\mathbf{x}_i))$. In equation (15), $\{\gamma_i\}_{i \in \mathcal{J}}$ are independent Rademacher random variables owing to their construction. Equation (16) can be derived from Theorem 1. Thus, combining equations (12), (13), and (17), we conclude that, with probability of at least $1 - e^{-2L\delta^2}$,

$$\sup_{V \in \mathcal{V}_d} \sum_{\ell=1}^L \mathbb{1} \{ (P - P_{B_\ell}) \xi_V > \epsilon \} \leq L \left(\frac{4}{B\epsilon^2} \mu_4 + \frac{|\mathcal{O}|}{L} + \frac{8}{N\epsilon} \sqrt{d\mu_4 |\mathcal{I}|} + \delta \right). \tag{18}$$

We choose $\delta = \frac{2}{4+\eta} - \frac{|\mathcal{O}|}{L}$ and

$$\epsilon = 2 \max \left\{ \sqrt{\frac{8(4+\eta)\mu_4}{\eta}} \sqrt{\frac{L}{N}}, \frac{16\sqrt{d\mu_4}(4+\eta)}{\eta} \frac{\sqrt{|\mathcal{I}|}}{N} \right\}.$$

The right hand side of (18) thus becomes strictly lesser than $\frac{L}{2}$. Thus, we have shown that

$$\mathbb{P} \left(\sup_{V \in \mathcal{V}_d} (P\xi_V - \text{MoM}_L^N(\xi_V)) > \epsilon \right) \leq e^{-2L\delta^2}.$$

Similarly, we can show that,

$$\mathbb{P} \left(\sup_{V \in \mathcal{V}_d} (\text{MoM}_L^N(\xi_V) - P\xi_V) > \epsilon \right) \leq e^{-2L\delta^2}.$$

Merging the above two inequalities, we obtain:

$$\mathbb{P} \left(\sup_{V \in \mathcal{V}_d} |\text{MoM}_L^N(\xi_V) - P\xi_V| > \epsilon \right) \leq 2e^{-2L\delta^2}.$$

Alternatively, with at least probability $1 - 2e^{-2L\delta^2}$,

$$\sup_{V \in \mathcal{V}_d} |\text{MoM}_L^N(\xi_V) - P\xi_V| \leq 2 \max \left\{ \sqrt{\frac{16(2+\eta)\mu_4}{\eta}} \sqrt{\frac{L}{N}}, \frac{32\sqrt{d\mu_4}(2+\eta)}{\eta} \frac{\sqrt{|\mathcal{I}|}}{N} \right\}$$

$$\leq C\sqrt{\mu_4} \left(\sqrt{\frac{L}{N}} + \frac{\sqrt{d|\mathcal{I}|}}{N} \right).$$

□

From Theorem 2, we can say that for any $V \in \mathcal{V}_d$, $\text{MoM}_L^N(\xi_V)$ and $P\xi_V$ are close to each other with a high probability. Thus, one can expect their corresponding minimum values to be close enough with a high probability. Theorem 3 affirms this claim. We show that $\mathfrak{R}(\hat{V}_d) \lesssim \sqrt{\mathbb{E}\|\mathbf{x}\|^4} \left(\sqrt{\frac{L}{N}} + \frac{\sqrt{d|\mathcal{I}|}}{N} \right)$ with a high probability.

Theorem 3. Under A1–3, and $N > L$, with probability at least, $1 - 2e^{-2L\left(\frac{2}{4+\eta} - \frac{|\mathcal{O}|}{L}\right)^2}$,

$$\mathfrak{R}(\hat{V}_d) \leq 2C\sqrt{\mathbb{E}\|\mathbf{x}\|^4} \left(\sqrt{\frac{L}{N}} + \frac{\sqrt{d|\mathcal{I}|}}{N} \right),$$

where C is defined as in Theorem 2.

Proof. Using the bound derived in equation (5), we observe the following:

$$\mathfrak{R}(\hat{V}_d) \leq 2 \sup_{V \in \mathcal{V}_d} |\text{MoM}_L^N(\xi_V) - P\xi_V| \leq 2C\sqrt{\mathbb{E}\|\mathbf{x}\|^4} \left(\sqrt{\frac{L}{N}} + \frac{\sqrt{d|\mathcal{I}|}}{N} \right). \quad (19)$$

From Theorem 2, equation (19) holds with probability at least $1 - 2e^{-2L\left(\frac{2}{4+\eta} - \frac{|\mathcal{O}|}{L}\right)^2}$, proving the desired result. □

3.4 Inference for Real Vector Spaces

In this section, we discuss the main implications of Theorem 3 for real vector spaces. We consider the special case of $\mathcal{H} = \mathbb{R}^p$. We observe that $\frac{2}{4+\eta} - \frac{|\mathcal{O}|}{L} \geq \frac{2}{4+\eta} - \frac{1}{2+\eta} = \frac{\eta}{(2+\eta)(4+\eta)} > 0$. Thus, if $L \rightarrow \infty$, $1 - 2e^{-2L\left(\frac{2}{4+\eta} - \frac{|\mathcal{O}|}{L}\right)^2} \rightarrow 1$. We note that,

$$\mathfrak{R}(\hat{V}_d) \lesssim \sqrt{\mathbb{E}\|\mathbf{x}\|^4} \left(\sqrt{\frac{L}{N}} + \frac{\sqrt{d|\mathcal{I}|}}{N} \right).$$

If each component of the inliers were generated independently from the same distribution, it is easy to observe that, $\mathbb{E}\|\mathbf{x}\|^4 \asymp p^2$. Thus, it is only natural to make the following assumption about P .

A4. $\mathbb{E}_{\mathbf{x} \sim P} \|\mathbf{x}\|^4 = \Theta(p^2)$.

Thus, with a high probability,

$$\mathfrak{R}(\hat{V}_d) \lesssim p \left(\sqrt{\frac{L}{N}} + \frac{\sqrt{d|\mathcal{I}|}}{N} \right) \leq p \left(\sqrt{\frac{L}{N}} + \sqrt{\frac{d}{N}} \right).$$

In other words, if $L = o\left(\frac{N}{p^2}\right)$ and $p^2d = o(N)$, then $\mathfrak{R}(\hat{V}_d) \rightarrow 0$, with probability tending to 1.

To formally state this result, we make the following two assumptions.

A5. $L \rightarrow \infty$, as $N \rightarrow \infty$.

A6. $p^2L, p^2d = o(N)$.

Such conditions apply naturally: as n increases, so too must L to preserve a proportion of the outlier-free partitions. Besides, the increase of L should be slower than n so that each partition can be assigned with sufficient data points. Note that since $d \leq p$, if $p^3 = o(N)$, then the second part of assumption 6 is satisfied. In other words, N has to increase faster than the cube of the feature space dimensions. The condition implied by A6 i.e., $|\mathcal{O}| = o(n)$ is intuitively appealing, and widely accepted [35, 36] as the number of outliers should be small by definition.

Before we state our result in Corollary 1, we recall that $X_n = O_P(a_n)$ if the sequence of random variables $\{X_n/a_n\}_{n \in \mathbb{N}}$ is tight [53].

Corollary 1. *Then under, A1-6, $\mathfrak{R}(\hat{V}_d) = O_P\left(p\left(\sqrt{\frac{L}{N}} + \sqrt{\frac{d}{N}}\right)\right)$ and $\mathfrak{R}(\hat{V}_d) \xrightarrow{P} 0$.*

Proof. We note that $\mathfrak{R}(\hat{V}_d) \lesssim p\left(\sqrt{\frac{L}{N}} + \sqrt{\frac{d}{N}}\right)$, with probability at least $1 - 2e^{-2L\left(\frac{2}{4+\eta} - \frac{|\mathcal{O}|}{L}\right)^2}$. By A3 and 6, $2e^{-2L\left(\frac{2}{4+\eta} - \frac{|\mathcal{O}|}{L}\right)^2} = o(1)$. Thus, $\mathbb{P}\left(\mathfrak{R}(\hat{V}_d) = O\left(p\left(\sqrt{\frac{L}{N}} + \sqrt{\frac{d}{N}}\right)\right)\right) \geq 1 - o(1)$. Hence,

$$|Pf_{\hat{Q}_{N,L}} - Pf_{Q^*}| = O_P\left(p\left(\sqrt{\frac{L}{N}} + \sqrt{\frac{d}{N}}\right)\right)$$

$$\text{Under A6, } p\left(\sqrt{\frac{L}{N}} + \sqrt{\frac{d}{N}}\right) = o(1) \implies \mathfrak{R}(\hat{V}_d) = o_P(1)^1. \quad \square$$

To conclude that $\hat{V}_d \xrightarrow{P} V_d^*$, we need to ensure that V_d^* is identifiable. Towards ensuring that, we make the following identifiability assumption on V_d^* . This type of identifiability conditions are especially popular in clustering literature [54, 55].

A7. For all $\epsilon > 0$, there exists $\delta > 0$, such that, if $\|V - V_d^*\| > \epsilon$, $\mathfrak{R}(V) \geq \delta$.

We will say that $V_n \rightarrow V$ if $\|V_n - V\| \rightarrow 0$. With this notion of convergence in the Frobenius sense, we are now ready to prove that \hat{V}_d is consistent for V_d^* .

Corollary 2. *Under A1-7, $\hat{V}_d \xrightarrow{P} V_d^*$.*

Proof. We fix $\epsilon > 0$. By A7, there exists $\delta > 0$, such that, if $\|\hat{V}_d - V_d^*\| > \epsilon$, $\mathfrak{R}(\hat{V}_d) \geq \delta$. Thus,

$$\mathbb{P}(\|\hat{V}_d - V_d^*\| > \epsilon) \leq \mathbb{P}\left(\mathfrak{R}(\hat{V}_d) \geq \delta\right) \rightarrow 0,$$

as $N \rightarrow \infty$, by appealing to Corollary 1. Thus, $\|\hat{V}_d - V_d^*\| \xrightarrow{P} 0 \iff \hat{V}_d \xrightarrow{P} V_d^*$. \square

Remark: Cost of Robustness The above results under our paradigm, the MoMPCA estimates admit an excess risk of $O\left(p\left(\sqrt{\frac{L}{N}} + \sqrt{\frac{d}{N}}\right)\right)$. We observe that since $L \geq 1$, $p\left(\sqrt{\frac{L}{N}} + \sqrt{\frac{d}{N}}\right) = \Omega(n^{-1/2})$. Thus, our framework's convergence rate for MoMPCA is generally slower than its ERM counterpart, which has a rate of $O(n^{-1/2})$. This reiterates that there is “no free lunch” when compromising robustness for the convergence rate, which is not unusual given that MoM operates on data contaminated with outliers. However, if the number of partitions L increases slowly compared to n (say, $L = O(\log n)$ and $|\mathcal{O}| = O(\log n)$), the excess risk for MoMPCA estimates draws closer to its ERM counterpart at a rate of $\tilde{O}(n^{-1/2})$.

Remark: Choice of L If the number of partitions can mitigate the effect of the outliers, under the proposed framework, the excess risk of the robust MoM estimates decreases with the

¹ $X_n = o_P(a_n)$ if $X_n/a_n \xrightarrow{P} 0$ [53].

block size at the rate of b as $1/\sqrt{b} = \sqrt{L/n}$. Since L can identify approximately as $2|\mathcal{O}|$, the corresponding excess risk has the rate of $O(\sqrt{|\mathcal{O}|/n})$. However, the error bound $O(\sqrt{|\mathcal{O}|/n})$ becomes vacuous if $|\mathcal{O}| \propto n$. Thus, it is essential that $|\mathcal{O}| = o(n)$ for our consistency guarantees to hold, as this enables us to select L satisfying A5-6. One should note that one can achieve an error rate of $O(n^{(\beta-1)/2})$ if $|\mathcal{O}| = O(n^\beta)$, for some $0 < \beta < 1$.

Remark: Comparison with MCM-PCA The recent array of works on geometric median-based approaches provide an attractive alternative to our proposal [18, 19, 20, 21]. However, the two approaches are significantly different. The geometric median-based approaches focus on finding a robust estimate of the dispersion matrix using a geometric median-based loss function. These approaches then go on to find a suitable subspace for low-dimensional representation of the data by an eigen decomposition of this robust estimate of the covariance matrix. On the other hand, MoMPCA approaches changing the ERM problem and introducing a robust estimate of the projection error. Theoretically, we derive finite-sample error bounds in Hilbert space without imposing any assumption on the outliers, thus relaxing the i.i.d. assumption of the data distribution imposed in [19].

Remark The MoMPCA method proposed in the paper can provide a more accurate analysis of data with outliers compared to existing methods. This is because the method is specifically designed to handle outlier data, and does not rely on unrealistic assumptions about the data distribution. The MoMPCA method does not make assumptions about the distribution of the outlier data. This allows for greater flexibility in dealing with different types of outlier behavior, making the method more useful in real-world applications where the nature of outliers may not be known in advance. Furthermore, the MoMPCA method provides a more interpretable understanding of PCA in the presence of outliers. This can be especially useful in applications where the insights provided by the analysis are important for decision-making. We note that MoMPCA does not require the data to have nice tail-conditions such as sub-Gaussian or sub-exponential behavior as required by many relevant works in this direction [24, 34], which are often unrealistic assumptions for real-world data. This means that the method can be applied to a wider range of datasets, making it more useful in practice.

4 Experimental Results

n	p	$\text{rank}(\mathbf{x}_0)$	PCP [7]	PCPF [12]	MFRPCA [56]	RWL-AN [8]	MCM-PCA [19]	MoMPCA (Proposed)
500	500	10	1.6×10^{-3}	1.5×10^{-3}	2.3×10^{-3}	8.7×10^{-3}	1.8×10^{-3}	1.5×10^{-3}
1000	500	10	7.3×10^{-4}	2.8×10^{-4}	1.8×10^{-3}	2.9×10^{-4}	2.7×10^{-4}	2.1×10^{-4}
2000	500	10	8.8×10^{-4}	1.1×10^{-4}	8.3×10^{-4}	3.1×10^{-4}	6.4×10^{-5}	5.6×10^{-5}
5000	500	10	2.1×10^{-4}	9.6×10^{-5}	5.7×10^{-4}	3.3×10^{-4}	8.1×10^{-6}	7.2×10^{-6}
10000	500	10	7.8×10^{-5}	8.2×10^{-5}	2.9×10^{-4}	9.5×10^{-5}	4.3×10^{-7}	3.8×10^{-7}

Table 1: Performance of different peer algorithms for low-rank matrix representation in terms of the relative reconstruction error.

In this section, we demonstrate the efficacy of MoMPCA on synthetic and natural datasets. We apply MoMPCA to perform different tasks, including low-rank matrix reconstruction in the presence of outliers, background modeling for video data, and anomaly detection for real data benchmarks. The codes and machine specifications are given at <https://github.com/SaptarshiC98/MOMPCA>.

Parameter Selection: The gradient descent parameter η used for the optimization here is typically chosen based on standard methods [57]. In our experiments, we fix η at 0.01. Thus, the only parameter to be selected is the number of partitions L . By the relationship $LB = n$, the block

n	p	$\text{rank}(\mathbf{x}_0)$	PCP [7]	PCPF [12]	MFRPCA [56]	RWL-AN [8]	MCM-PCA [19]	MoMPCA (Proposed)
500	500	10	106.05	104.13	106.81	8.14	2.34	5.18
1000	500	10	320.43	311.18	321.32	11.40	4.94	10.31
2000	500	10	952.87	932.65	956.05	26.76	10.35	21.27
5000	500	10	3203.54	3197.43	3215.29	49.03	21.02	53.28
10000	500	10	9608.68	9547.83	9677.04	103.42	45.96	98.04

Table 2: Runtime Comparison of different peer algorithms for low-rank matrix representation.

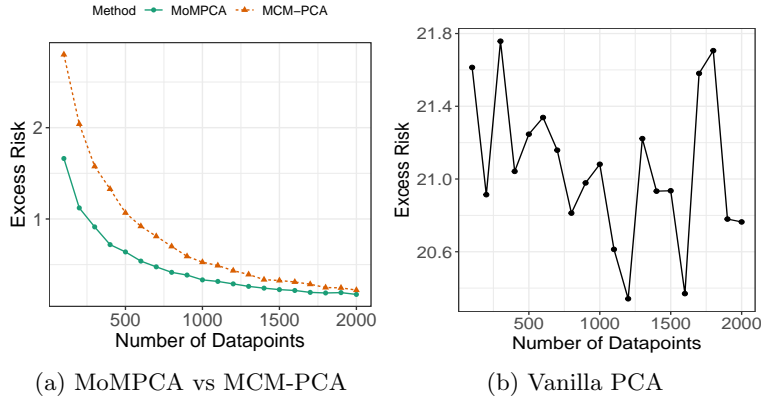


Figure 3: Comparison of excess risk of MoMPCA with MCM-PCA and vanilla PCA as discussed in Section 4.1. The vanilla PCA is shown in a different picture for a difference in scale.

size B is chosen automatically once L is fixed. For the PCA to be effective, the block size must be greater than p , which imposes an upper bound on L to be $\frac{n}{p}$. On the other hand, to maintain the parity with the theoretical results, we notice in assumption 3 that L must be greater than $2|\mathcal{O}|$, where $|\mathcal{O}|$ is the number of outliers present in the datapoint. This imposes a lower bound on L , and hence in ideal cases, L should be between $2|\mathcal{O}|$ and $\frac{n}{p}$. However, the number of outliers present in a dataset is typically unknown, and L must be greater than $2|\mathcal{O}|$ signifies a particular case where every partition contains exactly one outlier. In practice, since the partitions are done randomly, the probability of that happening is very low. Hence, we may select L to be much less than $2|\mathcal{O}|$. This relaxation in the choice of L leads to the possibility of using the MoMPCA algorithm for datasets where the number of outliers is quite large and $2|\mathcal{O}|$ surpasses the quantity $\frac{n}{p}$. Hence, in practice, we have chosen L to be less than $\frac{n}{p}$, with regard to being sufficiently large so that the median class can be free of outliers.

4.1 Simulation Study for Excess Risk Comparison

To empirically verify the efficacy of MoMPCA, we perform a simulation study to compare against vanilla PCA and the recently proposed MCM-PCA [19]. We generate the inlying observations of the dataset independently from $p = 10$ dimensional multivariate Gaussian distribution with mean $\mathbf{0}$ and covariance matrix $\Sigma = \text{diag}(10, 9, \dots, 2, 1)$. Thus, the first two dimensions are most important when projecting the entire data in a two-dimensional subspace. The outliers, which consist of 10% of datasets, are generated independently from multivariate Gaussian as well, with mean vector $(-20, 20, 0, 0, 0, 0, 0, 0, 0, 0)$ and I_{10} as the covariance matrix.

We then run all three algorithms on the datasets, starting with a total number of datapoints $n = 100$ to $n = 2000$, on a difference of 100. The experiments for each value of n are repeated 500 times. We then report the average value of the excess risk for the inliers, which is defined in Eq.

(4) takes the form as follows,

$$\begin{aligned} \mathfrak{R}(\hat{P}) &= \mathbb{E} \left(\|P_0 \mathbf{x}\|^2 - \|\hat{P} \mathbf{x}\|_2^2 \right) = \mathbb{E} \left(\mathbf{x}^\top (P_0 - \hat{P}) \mathbf{x} \right) = \mathbb{E} \text{Trace} \left(\mathbf{x}^\top (P_0 - \hat{P}) \mathbf{x} \right) \\ &= \mathbb{E} \text{Trace} \left((P_0 - \hat{P}) \mathbf{x} \mathbf{x}^\top \right) \\ &= \text{Trace} \left((P_0 - \hat{P}) \Sigma \right) \end{aligned}$$

We calculate the excess risk for each algorithm, where P_0 is the actual projection matrix for projecting onto the first two-dimension and \hat{P} is the projection matrix estimated by the respective algorithms. Then, we plot the average value of test error for each of the 3 algorithms and compare them in Fig. 3. We can clearly see that the proposed MoMPCA algorithm performs the best among its peers in terms of test error. In Fig. 3, we show the excess risk of MoMPCA and MCM-PCA in the same subfigure since both have a similar decay rate, with MoMPCA consistently better. On the other hand, the vanilla PCA falls apart and has an excess risk much more significant than its peers. Additionally, one should note that the rate of decrease in the excess risk resembles the risks derived in Corollary 1, validating the theoretical analysis in the process.

4.2 A Simulation Study on Recovering Low-rank Matrices

To empirically validate the efficacy of MoMPCA, we performed this dimensionality reduction procedure on various simulated datasets. We have generated the matrix \mathbf{x}_0 as a product of two matrices $\mathbf{x}_{1,0}$ and $\mathbf{x}_{2,0}$ of orders $n \times r$ and $r \times p$ respectively where each entry is simulated from the Gaussian distribution, where r is the rank of \mathbf{x}_0 and $r < \min\{n, p\}$. To add outliers, we add random noise generated from $Unif(-500, 500)$ to randomly selected \sqrt{n} many rows of \mathbf{x}_0 .

We then run the MoMPCA algorithm along with the peer algorithms on \mathbf{x}_0 . We calculate the efficacy of each of the relative reconstruction errors as $\frac{\|\mathbf{x} - \mathbf{x}_0\|}{\|\mathbf{x}_0\|}$, where the norm is taken over those rows that do not contain an outlier. Here X is the projected matrix in the lower d -dimensional affine space. Clearly, a lower score represents a better representation in lower-dimensional space. Since the true structure of the matrix lies in a lower-dimensional space, the MoMPCA method successfully plots the dataset in a lower-dimensional space despite having \sqrt{n} many outliers due to its robustness property.

We compare our method with the baselines as well as state-of-the-art methods such as Principal Component Pursuit (PCP) [7], Principal Component Pursuit with Features (PCPF) [12], Matrix-Factorization Based Robust Principal Component Analysis (MFRPCA) [56] and Robust Weight Learning with Adaptive Neighbors (RWL-AN) [8]. The standard protocols used by each of the original papers of the competing algorithms have been implemented in our experiments. The algorithms providing non-deterministic output have been run 20 times, and the average values obtained have been reported. The results demonstrated in table 1 clearly indicate that out of all the methods, the proposed MoMPCA algorithm works best in terms of the reconstruction error.

Runtime Analysis: We run each of the algorithms as demonstrated in section 4.2 and compare their total runtime. In table 2, the total time in seconds needed to run the algorithms on an M1 Macbook Pro with 8 GB RAM and 256 GB storage is provided. As evident, the first three algorithms, namely PCP [7], PCPF and MFRPCA are all matrix-factorization-based algorithms and hence take a huge amount of time to run as compared to the rest. The proposed algorithm MoMPCA is run for 50 iterations since the algorithm mostly converges much before. We can clearly see from the runtime analysis that the time required to run MoMPCA is almost equivalent to that of MCM-PCA while providing a better performance against the outliers.

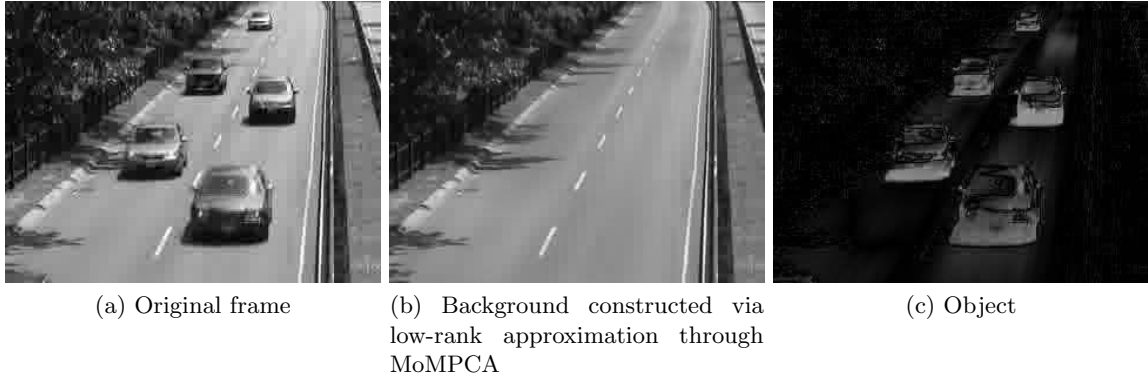


Figure 4: Background modeling through MoMPCA. The background is modeled as a low-dimensional approximation, calculated through MoMPCA as described in section 4.3.

Data	# Dimensions	# Instances	Anomaly ratio
KDDCUP	120	494,021	0.2
Thyroid	6	3,772	0.025
Arrhythmia	274	452	0.15

Table 3: Statistics of different anomaly detection benchmarks

4.3 Background Modeling in Video

Suppose we are given a video with f many frames. The objective here is to isolate the moving objects in the video, such as moving cars, pedestrians, etc. For simplicity, we only consider black and white videos (and thus, there is only a single channel) and let each frame be of size $m \times n$. We construct $\mathcal{X} = \{\mathbf{x}_1, \dots, \mathbf{x}_{mn}\} \subset \mathbb{R}^f$ by computing a $f \times 1$ vector whose features represent the value of a particular pixel for each frame. Since consecutive frames are highly correlated, one can expect that the data cloud \mathcal{X} lies near a low-dimensional affine space in \mathbb{R}^f . Thus, the background of the video can be modeled as the projection of \mathcal{X} on this low-dimensional affine space. To demonstrate the efficacy of modeling the background through MoMPCA, we take the standard video, called “highway” (available in the github repository), which captures moving cars on a busy highway. The video contains 1700 frames, and each frame is of size 240×320 . We construct a 76800×1700 data matrix whose rows denote the data points. We run the MoMPCA with $L = 40$ and $d = 5$. The background is thus given by $\{\mathbf{Q}\mathbf{x}_1, \dots, \mathbf{Q}\mathbf{x}_{76800}\}$, where \mathbf{Q} is the projection matrix, given by Algorithm 1. The output background for frame no. 863 is shown in Fig. 4 along with the original frame. The object is constructed by taking $\{\|\mathbf{x}_i - \mathbf{Q}\mathbf{x}_i\|_1\}_{i=1}^{76800}$. The object conforms to the moving cars in the original frame, and the background only consists of the highway and motionless trees.

4.4 An application in Anomaly Detection

Anomaly or outlier detection is a key problem in machine learning and computer vision. In this section, we will focus on how to detect outliers through MoMPCA. Suppose $\mathcal{X} = \{\mathbf{x}_1, \dots, \mathbf{x}_n\} \subset \mathbb{R}^p$ be n data points in the p -dimensional real vector space. To detect outliers within the data, we first project \mathcal{X} to a d -dimensional affine space via MoMPCA. We then compute the squared Euclidean distance between the original and projected data points $v_i = \|\mathbf{x}_i - \widehat{\mathbf{Q}}_{N,L}\mathbf{x}_i\|^2$ and sort v_i ’s in ascending order. We call the i -th point an outlier if v_i belongs to the largest $o\%$ of the $\{v_i\}_{i=1}^n$, where o is known beforehand.

Method	KDDCUP			Thyroid			Arrhythmia			Average
	Precision	Recall	F_1	Precision	Recall	F_1	Precision	Recall	F_1	rank (F_1)
OC-SVM [58]	0.7457	0.8523	0.7954	0.3639	0.4239	0.3887	0.5397	0.4082	0.4581	6.67
DSEBM-r [59]	0.8521	0.6472	0.7328	0.0404	0.0403	0.0403	0.1515	0.1513	0.1510	13.33
DSEBM-e [59]	0.8619	0.6446	0.7399	0.1319	0.1319	0.1319	0.4667	0.4565	0.4601	9.00
DCN [60]	0.7696	0.7829	0.7762	0.3319	0.3196	0.3251	0.3758	0.3907	0.3815	8.67
GMM-EN [61]	0.1932	0.1967	0.1949	0.0213	0.0227	0.0220	0.3000	0.2792	0.2886	14.33
PAE [61]	0.7276	0.7397	0.7336	0.1894	0.2062	0.1971	0.4393	0.4437	0.4403	10.33
E2E-AE [61]	0.0024	0.0025	0.0024	0.1064	0.1316	0.1176	0.4667	0.4538	0.4591	11.67
PAE-GMM-EM [61]	0.7183	0.7311	0.7246	0.4745	0.4538	0.4635	0.3970	0.4168	0.4056	10.00
PAE-GMM [61]	0.7251	0.7384	0.7317	0.4532	0.4881	0.4688	0.4575	0.4823	0.4684	7.17
DAGMM-p [61]	0.7579	0.7710	0.7644	0.4723	0.4725	0.4713	0.4909	0.4679	0.4787	4.67
DAGMM-NVI [61]	0.9290	0.9447	0.9368	0.4383	0.4587	0.4470	0.5091	0.4892	0.4981	4.00
DAGMM [61]	0.9297	0.9442	0.9369	0.4766	0.4834	0.4782	0.4909	0.5078	0.4983	1.67
RSPCA [62]	0.8503	0.6587	0.7480	0.4532	0.4881	0.4688	0.3523	0.3765	0.3706	8.50
SPCA-Barron [63]	0.7523	0.7602	0.7657	0.2245	0.2361	0.2398	0.4327	0.4592	0.4516	8.33
MoMPCA (Proposed)	0.8966	0.9106	0.9035	0.6974	0.5699	0.6272	0.5469	0.5303	0.5385	1.67

Table 4: Performance of different peer algorithms for anomaly detection. The average ranks based on the F_1 scores are also reported. The best performances for each data w.r.t. each metric are boldfaced.

For our comparative analysis, we take the KDDCUP, Thyroid, and Arrhythmia datasets, available from the UCI machine learning repository [64] and ODDS library [65]. The details of these datasets are reported in Table 3. We compared our method with different state-of-the-art techniques for outlier detection including OC-SVM [58]; DSEBM-e & DSEBM-r [59]; DCN [60]; GMM-EN, PAE, E2E-AE, PAE-GMM-EM, PAE-GMM, DAGMM-p, DAGMM-NVI, DAGMM [61], RSPCA [62] and Stochastic PCA with Barron loss [63]. Many competing algorithms employ a deep neural network to detect anomalies within the data. To measure the performance of the peer algorithms, we take the average precision, recall, and F_1 score between the ground truth and the obtained labeling (inlier/outlier) of the data points. These measures of accuracy for all three datasets are reported in Table 4. The performance indicator values for the peer algorithms are quoted from [61]. It is observed from Table 4 that the MoMPCA is quite competitive against state-of-the-art anomaly detection methods, including even the ones based on deep neural networks.

5 Conclusion

Despite the efficacy, computational simplicity, and ease of visualization of the classical PCA, it often fails to successfully represent the true low-dimensional structure of a dataset in the presence of even a small number of outliers. The traditional approach to formulating robust principal component analysis (PCA) assumes that the data matrix can be decomposed into a low-rank signal component and a noise component. However, this framework is not suitable when dealing with outliers that follow arbitrary distributions and/or are correlated to each other.

This paper proposes an alternative PCA method based on the Median of Means (MoM) estimator to circumvent this problem. The eigen-decomposition trick for PCA cannot be applied in this context, so we use an alternative approach involving projected Adagrad. The proposed MoMPCA, equipped with a computationally simple gradient descent-based optimization procedure, exhibits significant robustness to the presence of outliers. Under minimal and interpretable assumptions, we establish the consistency of MoMPCA in a general separable Hilbert space and find the convergence rate using uniform concentration bounds. The paper’s theoretical analysis is carried out with the aid of symmetrization arguments and Rademacher complexities, which, although extensively used

in a supervised learning setting, seldom find application in an unsupervised learning scenario. The parametric rates for real vector spaces can easily be recovered by taking the Hilbert space to be \mathbb{R}^p . The applicability of our theoretical results to an infinite-dimensional Hilbert space to derive dimension-free bounds with minimal assumptions, is not only novel but also opens up exciting avenues for future research in robust kernel-based methods.

Through practical applications in computer vision, MoMPCA is shown to be compelling relative to even some of the recent deep learning models. The robustness of MoM estimators comes at the expense of slower convergence rates than their ERM counterparts, as demonstrated in the paper. We stress the fact that there is *no wizardry in the median of means estimator* and that the interplay between the partitions and the outliers determines how effective MoM is. A potential future extension of our work could be to make the optimization faster by using adaptive gradient-based optimizers and proving their convergence properties. Future research in this direction might render fruitful avenues in improving the “slow” ERM rates by establishing fast rates under more restrictive assumptions [66, 67] or finding lower bounds on the approximation error.

References

- [1] Karl Pearson. Liii. on lines and planes of closest fit to systems of points in space. *The London, Edinburgh, and Dublin Philosophical Magazine and Journal of Science*, 2(11):559–572, 1901.
- [2] Svante Wold, Kim Esbensen, and Paul Geladi. Principal component analysis. *Chemometrics and intelligent laboratory systems*, 2(1-3):37–52, 1987.
- [3] Trevor Hastie, Robert Tibshirani, and Jerome Friedman. *The elements of statistical learning: data mining, inference, and prediction*. Springer Science & Business Media, 2009.
- [4] Michael E Tipping and Christopher M Bishop. Probabilistic principal component analysis. *Journal of the Royal Statistical Society: Series B (Statistical Methodology)*, 61(3):611–622, 1999.
- [5] Bernhard Schölkopf, Alexander Smola, and Klaus-Robert Müller. Kernel principal component analysis. In *International conference on artificial neural networks*, pages 583–588. Springer, 1997.
- [6] Hui Zou, Trevor Hastie, and Robert Tibshirani. Sparse principal component analysis. *Journal of computational and graphical statistics*, 15(2):265–286, 2006.
- [7] Emmanuel J Candès, Xiaodong Li, Yi Ma, and John Wright. Robust principal component analysis? *Journal of the ACM (JACM)*, 58(3):1–37, 2011.
- [8] Rui Zhang and Hanghang Tong. Robust principal component analysis with adaptive neighbors. In *Advances in Neural Information Processing Systems*, volume 32, pages 6961–6969, 2019.
- [9] John Wright, Arvind Ganesh, Shankar Rao, Yigang Peng, and Yi Ma. Robust principal component analysis: Exact recovery of corrupted low-rank matrices via convex optimization. In *Advances in Neural Information Processing Systems*, volume 22, pages 2080–2088, 2009.
- [10] Venkat Chandrasekaran, Sujay Sanghavi, Pablo A Parrilo, and Alan S Willsky. Rank-sparsity incoherence for matrix decomposition. *SIAM Journal on Optimization*, 21(2):572–596, 2011.

- [11] Zhao Kang, Chong Peng, and Qiang Cheng. Robust pca via nonconvex rank approximation. In *2015 IEEE International Conference on Data Mining*, pages 211–220. IEEE, 2015.
- [12] Kai-Yang Chiang, Cho-Jui Hsieh, and Inderjit Dhillon. Robust principal component analysis with side information. In *Proceedings of The 33rd International Conference on Machine Learning*, volume 48 of *Proceedings of Machine Learning Research*, pages 2291–2299, New York, New York, USA, 20–22 Jun 2016. PMLR.
- [13] Jicong Fan and Tommy W. S. Chow. Exactly robust kernel principal component analysis. *IEEE Transactions on Neural Networks and Learning Systems*, 31(3):749–761, 2020. doi: 10.1109/TNNLS.2019.2909686.
- [14] Shuangyan Yi, Zhenyu He, Xiao-Yuan Jing, Yi Li, Yiu-Ming Cheung, and Feiping Nie. Adaptive weighted sparse principal component analysis for robust unsupervised feature selection. *IEEE Transactions on Neural Networks and Learning Systems*, 31(6):2153–2163, 2020. doi: 10.1109/TNNLS.2019.2928755.
- [15] Gongguo Tang and Arye Nehorai. Robust principal component analysis based on low-rank and block-sparse matrix decomposition. In *2011 45th Annual Conference on Information Sciences and Systems*, pages 1–5. IEEE, 2011.
- [16] Namrata Vaswani, Thierry Bouwmans, Sajid Javed, and Praneeth Narayanamurthy. Robust subspace learning: Robust pca, robust subspace tracking, and robust subspace recovery. *IEEE signal processing magazine*, 35(4):32–55, 2018.
- [17] Qianqian Wang, Quanxue Gao, Xinbo Gao, and Feiping Nie. Angle principal component analysis. In *IJCAI*, pages 2936–2942, 2017.
- [18] Hervé Cardot, Peggy Cénac, and Pierre-André Zitt. Efficient and fast estimation of the geometric median in hilbert spaces with an averaged stochastic gradient algorithm. *Bernoulli*, 19(1):18–43, 2013.
- [19] Hervé Cardot and Antoine Godichon-Baggioni. Fast estimation of the median covariation matrix with application to online robust principal components analysis. *Test*, 26(3):461–480, 2017.
- [20] Heinrich Fritz, Peter Filzmoser, and Christophe Croux. A comparison of algorithms for the multivariate l 1-median. *Computational Statistics*, 27(3):393–410, 2012.
- [21] Michael B Cohen, Yin Tat Lee, Gary Miller, Jakub Pachocki, and Aaron Sidford. Geometric median in nearly linear time. In *Proceedings of the forty-eighth annual ACM symposium on Theory of Computing*, pages 9–21, 2016.
- [22] Vladimir Vapnik. *The nature of statistical learning theory*. Springer science & business media, 2013.
- [23] Gábor Lugosi, Shahar Mendelson, et al. Regularization, sparse recovery, and median-of-means tournaments. *Bernoulli*, 25(3):2075–2106, 2019.
- [24] Guillaume Lecué, Matthieu Lerasle, et al. Robust machine learning by median-of-means: theory and practice. *Annals of Statistics*, 48(2):906–931, 2020.

- [25] Peter L Bartlett, Stéphane Boucheron, and Gábor Lugosi. Model selection and error estimation. *Machine Learning*, 48(1):85–113, 2002.
- [26] Guillaume Lecué, Matthieu Lerasle, and Timlothée Mathieu. Robust classification via mom minimization. *Machine Learning*, 109(8):1635–1665, 2020.
- [27] Matthieu Lerasle. Lecture notes: Selected topics on robust statistical learning theory. *arXiv preprint [arXiv:1908.10761](https://arxiv.org/abs/1908.10761)*, 2019.
- [28] Pierre Laforgue, Stéphan Cléménçon, and Patrice Bertail. On medians of (randomized) pairwise means. In *International Conference on Machine Learning*, pages 1272–1281. PMLR, 2019.
- [29] Timothée Mathieu and Stanislav Minsker. Excess risk bounds in robust empirical risk minimization. *Information and Inference: A Journal of the IMA*, 2021.
- [30] Sébastien Bubeck, Nicolo Cesa-Bianchi, and Gábor Lugosi. Bandits with heavy tail. *IEEE Transactions on Information Theory*, 59(11):7711–7717, 2013.
- [31] Stanislav Minsker. Uniform bounds for robust mean estimators. *arXiv preprint [arXiv:1812.03523](https://arxiv.org/abs/1812.03523)*, 2018.
- [32] Yegor Klochkov, Alexey Kroshnin, and Nikita Zhivotovskiy. Robust k -means clustering for distributions with two moments. *arXiv preprint [arXiv:2002.02339](https://arxiv.org/abs/2002.02339)*, 2020.
- [33] Camille Brunet-Saumard, Edouard Genetay, and Adrien Saumard. K-bmom: a robust lloyd-type clustering algorithm based on bootstrap median-of-means. *arXiv preprint [arXiv:2002.03899](https://arxiv.org/abs/2002.03899)*, 2020.
- [34] Debolina Paul, Saptarshi Chakraborty, Swagatam Das, and Jason Xu. Uniform concentration bounds toward a unified framework for robust clustering. *Advances in Neural Information Processing Systems*, 34:8307–8319, 2021.
- [35] Guillaume Lecué, Matthieu Lerasle, and Timlothée Mathieu. Robust classification via mom minimization. *Machine Learning*, 109(8):1635–1665, 2020.
- [36] Guillaume Staerman, Pierre Laforgue, Pavlo Mozharovskiy, and Florence d’Alché Buc. When ot meets mom: Robust estimation of wasserstein distance. In Arindam Banerjee and Kenji Fukumizu, editors, *Proceedings of The 24th International Conference on Artificial Intelligence and Statistics*, volume 130 of *Proceedings of Machine Learning Research*, pages 136–144. PMLR, 13–15 Apr 2021. URL <http://proceedings.mlr.press/v130/staerman21a.html>.
- [37] Peter L Bartlett and Shahar Mendelson. Rademacher and gaussian complexities: Risk bounds and structural results. *Journal of Machine Learning Research*, 3(Nov):463–482, 2002.
- [38] Luc Devroye, László Györfi, and Gábor Lugosi. *A probabilistic theory of pattern recognition*, volume 31. Springer Science & Business Media, 2013.
- [39] Guillaume Lecué, Matthieu Lerasle, and Timlothée Mathieu. Robust classification via mom minimization. *Machine Learning*, 109(8):1635–1665, 2020.
- [40] Huishuai Zhang, Yi Zhou, and Yingbin Liang. Analysis of robust pca via local incoherence. *Advances in Neural Information Processing Systems*, 28, 2015.

- [41] Shenglan Liu, Lin Feng, and Hong Qiao. Scatter balance: An angle-based supervised dimensionality reduction. *IEEE transactions on neural networks and learning systems*, 26(2): 277–289, 2014.
- [42] Shenglan Liu and Yang Yu. Angular embedding: A new angular robust principal component analysis. *arXiv preprint arXiv:2011.11013*, 2020.
- [43] Soren Hauberg, Aasa Feragen, and Michael J Black. Grassmann averages for scalable robust pca. In *Proceedings of the IEEE Conference on Computer Vision and Pattern Recognition*, pages 3810–3817, 2014.
- [44] Søren Hauberg, Aasa Feragen, Raffi Enfciaud, and Michael J Black. Scalable robust principal component analysis using grassmann averages. *IEEE transactions on pattern analysis and machine intelligence*, 38(11):2298–2311, 2015.
- [45] Thierry Bouwmans, Sajid Javed, Hongyang Zhang, Zhouchen Lin, and Ricardo Otazo. On the applications of robust pca in image and video processing. *Proceedings of the IEEE*, 106(8): 1427–1457, 2018.
- [46] Quanxue Gao, Lan Ma, Yang Liu, Xinbo Gao, and Feiping Nie. Angle 2dpca: A new formulation for 2dpca. *IEEE transactions on cybernetics*, 48(5):1672–1678, 2017.
- [47] Quanxue Gao, Pu Zhang, Wei Xia, Deyan Xie, Xinbo Gao, and Dacheng Tao. Enhanced tensor rpca and its application. *IEEE transactions on pattern analysis and machine intelligence*, 43(6):2133–2140, 2020.
- [48] Shuangli Liao, Jin Li, Yang Liu, Quanxue Gao, and Xinbo Gao. Robust formulation for pca: Avoiding mean calculation with l_2 , p -norm maximization. In *Thirty-Second AAAI Conference on Artificial Intelligence*, 2018.
- [49] Guillaume Lecué and Matthieu Lerasle. Learning from mom’s principles: Le cam’s approach. *Stochastic Processes and Their Applications*, 129(11):4385–4410, 2019.
- [50] Daniela Rodriguez and Marina Valdora. The breakdown point of the median of means tournament. *Statistics & Probability Letters*, 153:108–112, 2019.
- [51] Raman Arora, Andrew Cotter, Karen Livescu, and Nathan Srebro. Stochastic optimization for pca and pls. In *2012 50th Annual Allerton Conference on Communication, Control, and Computing (Allerton)*, pages 861–868. IEEE, 2012.
- [52] Shai Shalev-Shwartz and Shai Ben-David. *Understanding machine learning: From theory to algorithms*. Cambridge university press, 2014.
- [53] Krishna B Athreya and Soumendra N Lahiri. *Measure theory and probability theory*. Springer Science & Business Media, 2006.
- [54] David Pollard. Strong consistency of k -means clustering. *Ann. Statist.*, 9(1):135–140, 01 1981. doi: 10.1214/aos/1176345339. URL <https://doi.org/10.1214/aos/1176345339>.
- [55] Saptarshi Chakraborty, Debolina Paul, Swagatam Das, and Jason Xu. Entropy weighted power k -means clustering. In *International Conference on Artificial Intelligence and Statistics*, pages 691–701. PMLR, 2020.

- [56] Yongyong Chen and Yicong Zhou. Robust principal component analysis with matrix factorization. In *2018 IEEE International Conference on Acoustics, Speech and Signal Processing (ICASSP)*, pages 2411–2415. IEEE, 2018.
- [57] Sebastian Ruder. An overview of gradient descent optimization algorithms. *arXiv preprint [arXiv:1609.04747](https://arxiv.org/abs/1609.04747)*, 2016.
- [58] Yunqiang Chen, Xiang Sean Zhou, and Thomas S Huang. One-class svm for learning in image retrieval. In *Proceedings 2001 International Conference on Image Processing (Cat. No. 01CH37205)*, volume 1, pages 34–37. IEEE, 2001.
- [59] Chao Zhang and Philip C Woodland. Joint optimisation of tandem systems using gaussian mixture density neural network discriminative sequence training. In *2017 IEEE International Conference on Acoustics, Speech and Signal Processing (ICASSP)*, pages 5015–5019. IEEE, 2017.
- [60] Bo Yang, Xiao Fu, Nicholas D Sidiropoulos, and Mingyi Hong. Towards k-means-friendly spaces: Simultaneous deep learning and clustering. In *international conference on machine learning*, pages 3861–3870. PMLR, 2017.
- [61] Bo Zong, Qi Song, Martin Renqiang Min, Wei Cheng, Cristian Lumezanu, Daeki Cho, and Haifeng Chen. Deep autoencoding gaussian mixture model for unsupervised anomaly detection. In *International Conference on Learning Representations*, 2018.
- [62] Jintang Bian, Dandan Zhao, Feiping Nie, Rong Wang, and Xuelong Li. Robust and sparse principal component analysis with adaptive loss minimization for feature selection. *IEEE Transactions on Neural Networks and Learning Systems*, 2022.
- [63] Mayur Dhanaraj and Panos P Markopoulos. Robust stochastic principal component analysis via barron loss. In *2022 56th Asilomar Conference on Signals, Systems, and Computers*, pages 1286–1290. IEEE, 2022.
- [64] Dheeru Dua and Casey Graff. UCI machine learning repository, 2017. URL <http://archive.ics.uci.edu/ml>.
- [65] Shebuti Rayana. ODDS library, 2016. URL <http://odds.cs.stonybrook.edu>.
- [66] Stéphane Boucheron, Olivier Bousquet, and Gábor Lugosi. Theory of classification: A survey of some recent advances. *ESAIM: Probability and Statistics*, 9:323–375, 2005.
- [67] Martin J Wainwright. *High-dimensional statistics: A non-asymptotic viewpoint*, volume 48. Cambridge University Press, 2019.